

Damage prediction in geothermal turbine blades based on the measurement of electrochemical noise.

J.A. Rodríguez¹, C.M. Clemente²

¹(Centro de Investigación en Ingeniería y Ciencias Aplicadas, (CIICAp), UAEM, Morelos, México)

Abstract: The geothermal turbine blades are critical components that convert the kinetic energy of the steam flow into mechanical energy. The blades of the last stage in low pressure are longer and they define the turbine's overall performance. Some problems of damage to the blades of low pressure, are caused by environment and particles into stage of steam turbine. These situation arise pitting corrosion in the surface of the blade and corrosion fatigue mechanisms. In this works the behavior of the material of the geothermal turbine blade which is made of stainless steel AISI 410 SS is described. The tests were conducted by exposing the blade material in a corrosive environment and load cycles causing damage corrosion fatigue, crack initiation and propagation. The corrosion fatigue phenomenon (CF) was studied through the electrochemical noise technique in potential. Crack formation of the pit was determined from the stress intensity factor was calculated assuming that the pit was a semi-elliptical crack.

Keywords -Pitting corrosion, corrosion fatigue, geothermal turbine blades and damage mechanisms.

I. INTRODUCTION

The low-pressure blades of geothermal turbines are critical components that need special attention into power plants. These blades generated between 10-12 % of total electrical energy of the turbine hence their importance. Previous research has shown that blades of LP are generally more susceptible to failure than blades of high pressure and intermediate pressure. The most common mechanisms of failure of these blades are normally associated with high vibration, steam flow imbalance, the cross between fundamental frequencies and harmonic. These situations generate repeated loads with high amplitudes that in consequence produce cracks in surface of the blades. These cracks combine with the environment of work originating as result accumulate corrosive ions and phenomena like erosion, corrosion, brittleness, stress corrosion and corrosion fatigue are presented. Failures by corrosion fatigue occur unexpectedly in power plants causing big economic losses [1-5].

The impurities in the steam such as chlorides and sulphates, Na, Fe, Cu, Si, PO₄ and CO₃ have varying concentrations in the vapor and in the working fluid [3]. It has been found that the blades exposed to environments containing sodium chloride and some iron compounds present some cracks. Crack initiation and propagation are important mechanisms of failure in blades due to pitting corrosion, which lead to a degradation process on the material surface [4-5]. An important condition for the safety of the blades of geothermal turbines is the assessment of the blades service life under corrosion fatigue conditions. The fracture mechanics plays an important role in information mechanical damage that occurs in blades. Therefore it is important to understand the corrosive environment in cracks when the material is exposed because there is a lot of information that can be used by damage detection and useful life estimation of blades under corrosion fatigue phenomena. In this regard, electrochemical techniques are used to determine the process of electrochemical reaction between the metal with cracks and without cracks in steady condition of operation. With this information damage can be detected and useful life calculated of geothermal turbine blades. Experimental and numerical models are used to predict damage and the life of geothermal turbine blades [6, 7]. In this work the corrosion rate of 410 stainless steel (SS 410) was experimentally determined in the presence of cracks as a function of time at room temperature. Numerical models were used by determined the stress intensity factor under these conditions and the useful life was calculated. The process involves damage calculated in four steps: nucleation pitting, pit growth, growth of short cracks and long cracks [8] [9] [10].

II. MATERIALS AND METHODS

2.1 Material

The test material was a steel AISI 410 SS grade martensitic 12% Cr - steel is a standard material for geothermal turbine blades low pressure. The chemical composition and mechanical properties are shown in Table 1 and 2.

2.2. Test specimens

The specimens were made according to ASTM E466 standard, for fatigue tests as shown in Figure 1, the results are expressed in terms of stress intensity ΔK defined for linear elasticity theory [11]. Samples for electrochemical testing were prepared as described in ASTM G01 and ASTM G1 standard [12] [13].

Table 1. Chemical composition AISI 410 SS (in wt%).

C	Cr	Mn	Si	Ni	Mo	Cu	S	P	Fe
0.13	12	0.41	0.22	0.33	0.18	0.09	0.002	0.020	Bal.

Table 2. Mechanical properties AISI 410 SS at room temperature.

Tensile strength (MPa)	Yield strength (MPa)	Elongation (A) %	Reduction of Area %
834	721	12	40

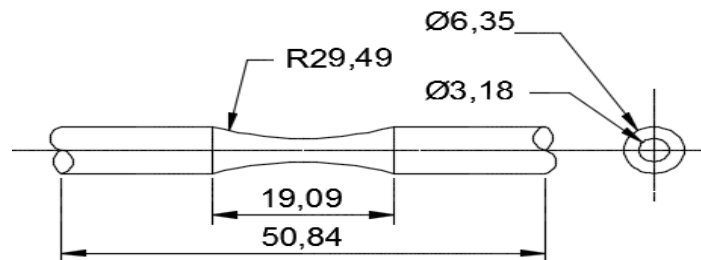


Fig 1. Dimensions of the specimen in mm.

2.3. Method corrosion fatigue test

The tests were conducted in a machine rotating bending fatigue RBF-200, where loads are applied between free bearings, producing the case of a simply supported beam subjected to pure bending [14]. In figure 2 shows the assembly made for corrosion fatigue tests shown. The specimen is located within an electrochemical cell containing closed 40 ml of 3% NaCl at room temperature electro platinum was used for the measurement potential via a potentiostat 1120 ACM model. The tests were conducted at a frequency of 20 Hz at 1200 RPM, four stress levels as shown in Table 3.

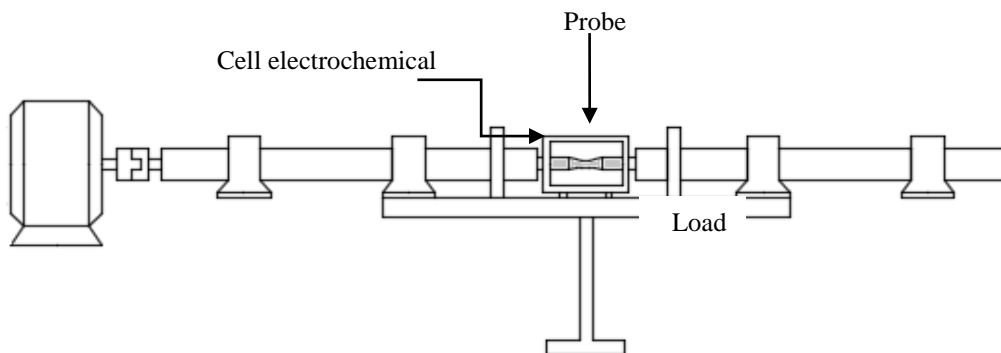


Fig 3. Machine rotating bending fatigue.

Table 3. Charges for corrosion fatigue tests.

SUT	Stress (MPa)	Momentum (N.m)
0.9	750.6	2.358
0.7	583.8	1.834

III. RESULT

3.1 Mathematical model

The total life of fatigue cracks is presented by the sum of these four phases by equation 1 [15]:

$$t_f = t_{pn} + t_{pg} + t_{sc} + t_{lc} \quad (1)$$

Table 4. Deterministic variable

Variable	Values
Density (g/m ³)	$\rho=7.8 \cdot 10^3$
Valence	n=3
Molecular weight (g)	$M=55.5 \cdot 10^{-3}$
Faraday's constant (C/mol)	F=96514
Activation Energy (kJ/mol)	$\Delta H=31 \cdot 10^3$
Universal gas constant (J/mol K)	R=8.314
Temperature (K)	T=363.15
Applied stress (MPa)	$\Delta S=834$
Frequency (cycles)	f=20
Stress concentration factor	$k_t=3$
Short crack growth exponent	$m_{sc}=3.40$
Long crack growth exponent	$m_{lc}=3.40$
Specified critical crack size (m)	$a_f=1 \cdot 10^{-2}$

Where TPN is the time for nucleation sting, t_{pn} is the time for growth sting t_{sc} is the time for growth and t_{lc} short crack is the time of long crack growth. The four phases based on deterministic variables were calculated from experimental tests and random variables were obtained from the method of first order reliability (FORM) and the method of reliability second order (SORM) shown in table 4. The probability of failure can be expressed by equation 2:

$$P_f = P(t_f - t < 0) = P_f(t_f \leq t) \quad (2)$$

3.2 Experimental model

In the Figures 4-5 electrochemical noise signals are shown in different levels of fatigue stress. They were obtained by exposing of steel specimens 410SS to solution of 3.0% NaCl at room temperature. It can

observed an increase and decrease in the potential signal in the time. This phenomenon is characteristic of the presence of pitting in the surface of the material. At the same time, a film protective oxide on the surface is formed, which acts as a barrier between the contact of the material surface and the solution. However, the protective film is damaged by loads applied due to the creation of slip bands micro-deformations and the formation of microcracks, therefore the process of anodic dissolution is carried out and the crack to propagate [16].

Figure 4 shows the time series of electrochemical noise under load cycle 750 MPa (90% σ_{ult}), at a frequency of 20 Hz and stress ratio $R = -1$. The series of potential obtained from electrochemical noise show a characteristic pattern of rapid decrease and slow recovery potential, where transients 70 and -20 mV are associated with the pit corrosion that could occur when a rupture of the passive layer is develops. On the other hand, the drop potential has a range of -25 to -150mV. This drop potential is related with the propagation of cracks [17].

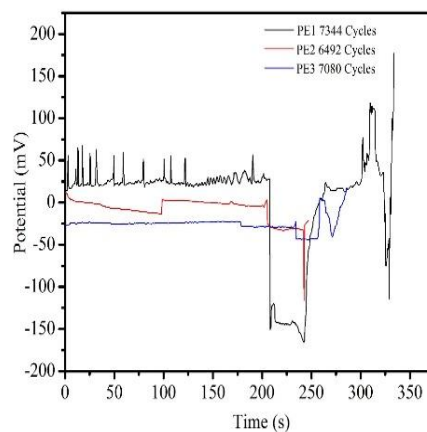


Fig 4. Behavior of AISI 410 SS steel in 3.0% NaCl at room temperature under induced load cycle $\Delta\sigma = 750$ MPa (90% σ_{ult}).

Figure 5. The time series of electrochemical noise under load cycle $\Delta\sigma = 583.8$ MPa (σ 70%) is at a frequency 20 Hz and stress ratio $R = -1$. Series potential obtained from electrochemical noise measurements show a common characteristic behavior between tests (31500 and 32640 cycles). A fast drop and slow recovery potential, where transients 20 and -20mV are associated with the pit of corrosion that can occur when a breakdown of the passive layer develops observed. Nevertheless the test cycles $N = 27972$, potential transients may result from the dissolution of the walls of the crack and a possible active solution over a period of time in

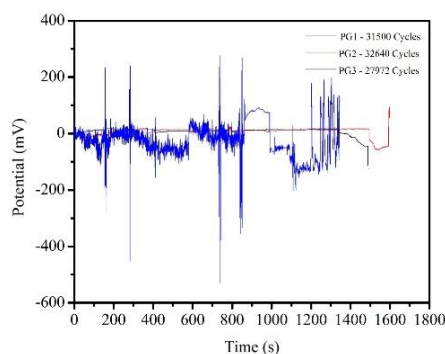


Fig 5. Behavior of AISI 410 SS steel in 3.0% NaCl at room temperature under induced load cycle $\Delta\sigma = 583.8$ MPa (70% σ_{ult}).

Generally the measurements electrochemical noise potential showed a common characteristic pattern of rapid potential drop followed by a short recovery voltage signal related to the pitting corrosion, passivation of the specimen during charging cycles, mechanically damaging the film protective during stripping slide, followed by a cracking process related to the anodic dissolution process. In Figure 6 the stress intensity factor (SIF) in the specimen according to the size of the crack shown. These data were used in the calculation for the growth of crack length. K_{max} results are shown in Table 5.

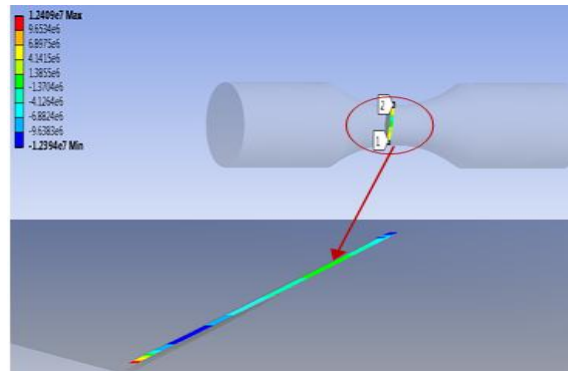


Fig 6. Stress Intensity Factor of specimen [19].

Table 6. Crack size

a	SIF	a	SIF
Experimental	Experimental	Simulated	Simulated
0.000144	4.178	0.000127	3.686
0.0000913	3.911	0.000114	4.876
0.0000962	3.787	0.000118	4.64
0.0000362	1.103	0.0000351	1.07
0.0000354	1.064	0.000035	1.052
0.0000329	1.025	0.0000276	0.86

IV. CONCLUSION

- Corrosion fatigue (CF) in the geothermal turbine blades is an important mechanism failure and leads to crack propagation. From the results obtained in tests using the corrosion fatigue electrochemical noise technique in potential it was possible to determine the mechanisms of corrosion, such as pitting nucleation to crack propagation on the material surface. The series of potential obtained from measurements in electrochemical noise show a common characteristic pattern of quick drop and slow recovery potential related to pitting corrosion, passivation of the specimen during charging cycles, affecting the protective passive layer during the creation of slip bands, followed by a cracking process related to the anodic dissolution process.
- Using the method of the first order (FORM) was possible to develop a mathematical model for predicting the fatigue life under corrosion fatigue phenomenon

REFERENCES

- [1] Mazur Z, Garcia R, Aguirre J and Perez N. (2008) Steam turbine blade failure Analysis. *Engineering Failure Analysis*, 15 (1-2) pg. 129-141.
- [2], Hyojn Kim. (2011) Crack evaluation of the fourth stage blade in a low pressure steam turbine. *Engineering Failure Analysis*. Vol.18.pg 907-913.
- [3], J.A. Rodríguez, Y.El. Hamzaoui, J.A. Hernández, J.C. García, J.E. Flores and A.L. Tejada. (2013). *Engineering Failure Analysis*. Pg. 562–575
- [4], Y.El. Hamzaoui, J.A. Rodríguez, Víctor Salazar. Optimization of operating conditions for steam turbine using an artificial neural network inverse. *Engineering Failure Analysis*. Vol. 75.Pg. 648-657.
- [5], J.A.Rodríguez , J.C García, E. Alonso. (2015). Failure probability estimation of steam turbine blades by enhanced Monte carlo method. *Engineering Failure Analysis*. Vol.56. Pg. 80-88
- [6] C. Cuevas Arteaga, J.A Rodríguez, C.M. Clemente, J.A. Segura, G. Urquiza, Y. EL. Hamzaoui. (2013). *Engineering Failure Analysis*.vol.35. Pg. 576-589.
- [7], Owen J and Fawkes A.J. (1983). *Engineering fracture mechanic. Numerical methods and application*.
- [8], Logan E and Roy R. (2003). *Handbook of turbomachinery third edition*.
- [9], Zhou S and Turnbull A. (1999). Influence of pitting on the fatigue life of a turbine steel. *Fatigue and Fracture of Engineering Materials and Structures* .Vol 22pp pg. 1083-1093.
- [10], Dooley R.B. (2007). Development of model to predict stress corrosion cracking and corrosion fatigue of a low pressure turbine components. Electric Power Research Institute.
- [11], Standard test method for measurement of fatigue crack growth rates ASTM E 647-88A (American society for testing and materials, 1988)
- [12], ASTM G1, 1991 (2011). Practice for preparing cleaning, and evaluation test specimen. West Conshohocken, PA: ASTM International
- [13] , ASTM G01 (1991) Corrosion metal.
- [14], RB 200 Instruction manual Model RBF-200: Rotating beam fatigue testing machine.
- [15], Ship P and Sankaran Mahadevan. (2001). Damage tolerance approach for probabilistic pitting corrosion fatigue life prediction. *Engineering Fracture Mechanics*. Pg. 1493-1507.
- [16], Acuña –González Narciso, González-Sánchez, Dzib-Pérez Luis R and Rivas-Menchi Aarón. (2012). Early corrosión fatigue damage on stainless Steel exposed to tropical seawater: A contribution from sensitive electrochemical techniques. *INTECH*. Pg. 229-259
- [17], González - Rodríguez, Salinas – Bravo V.M. Díaz - Sánchez A. (1997). Use of electrochemical potential noise to detect initiation and propagation of stress corrosion cracks in a 17-4PH Steel. *Corrosion Science*. Vol. 53. Pg.693-699.
- [18], Eiji Tada. (2007).Detection of corrosion fatigue cracking through current responses induced by cyclic stressing. *Corrosion Science*. Pg 248-254
- [19], C. Cuevas Arteaga, Rodríguez J.A, Clemente C.M, Rodríguez J.M, Mariaca Y. (2014). Pitting corrosion damage for prediction useful life of geothermal turbine blade. *American Journal of Mechanical Engineering*. Vol. 2. Pg. 164-168.